Journal of King Saud University – Engineering Sciences (2026) 38:26
https://doi.org/10.1007/s44444-025-00091-x

ORIGINAL PAPER

The evaluation of RSM optimization and kinetics modeling of essential oil extraction from *Citrus hystrix* leaves using microwave-assisted hydrodistillation

Dwi Setyorini[1] · Achmad Qodim Syafaatullah[1] · Sabdha Purna Yudha[1] · Frabowo Prasetya[1] · Anggi Yuktii Kulla[1] · Novita Ramadhani[1] · Silvana Zaimul[1] · Sitti Khusnul Khotimah[1]

Received: 28 April 2025 / Accepted: 6 December 2025 / Published online: 23 March 2026
© The Author(s) 2026

Abstract

This study explores the optimization and kinetic modeling of microwave-assisted hydrodistillation for essential oil extraction from *Citrus hystrix* leaves. There are three primary parameters of the microwave-assisted hydrodistillation method that were evaluated for their impact: power of microwave, feed to solvent (F/S) ratio, and time of extraction. The optimization extraction was analyzed by response surface methodology (RSM) using Box-Behnken design (BBD) and face-centered central composite design (FCCCD) models, and the quadratic model was the best fit to represent the experimental data. The optimum condition predicted using BBD was at 630 W, a F/S ratio of 0.35, and 135.788 min with a yield prediction of 1.367%. Whereas, the analysis using FCCCD was at 630 W, a F/S ratio of 0.35, and 150 min with a yield prediction of 1.426%. Kinetics modeling was carried out to determine the constant rate of extraction and maximum capacity of extraction, and the best suitable model was the first-order model. The values of R^2 and RSME were 0.9745 and 0.0556, respectively. FTIR analysis indicates that the essential oil extract has similarity (93.69%) with the citronellal compounds. GC–MS analysis was carried out to identify citronellal and citronellol compounds, whose contents were 70.39% and 14.33%, respectively. SEM analysis indicated the morphological structure of leaves damaged after extraction using microwave-assisted hydrodistillation. This damaged structure of leaves shows that the process of extraction destroys the cell wall structure of *Citrus hystrix* leaves. This study contributes valuable insight for improving and scaling up microwave-assisted hydrodistillation of essential oils from *Citrus hystrix* leaves.

Keywords Microwave-assisted hydrodistillation · *Citrus hystrix* leaves · RSM optimization · Kinetics models

1 Introduction

Essential oils are secondary molecules that are extracted from aromatic plants. They are extensively distributed in the roots, stems, leaves, flowers, fruits, and other plant parts and have a distinct scent (Drinić et al. 2020)–(Chen et al. 2020). It has been demonstrated that several *Citrus* species, including *Citrus hystrix* leaves, can be used as essential oils. Because of its powerful odor, *Citrus hystrix* essential oil has an excellent chance to develop further (Mohammadhosseini et al. 2017). Citronellal compounds make up the majority of the chemical content of *Citrus hystrix* leaves, which are also abundant in phytochemicals with carboxylic and phenolic functional groups (Golmohammadi et al. 2018; Ragab et al. 2019; Kusuma and Mahfud 2017). There are several biological uses for this essential oil of *Citrus hystrix* leaves, including fragrance, flavoring, spice, aromatherapy, antibacterial, and medical care (Megawati et al. 2019; Ngan et al. 2019).

Essential oils can be extracted through a variety of traditional and cutting-edge methods. Steam distillation, hydrodistillation, and organic solvent extraction are a few of the common and widely utilized methods (Drinić et al. 2020; Golmohammadi et al. 2018). Many drawbacks of the traditional approach stem from its working mechanism; these include losses in volatile components and bioactive substance content as well as an impact on the yield of essential oils (Chen et al. 2020)–(Ragab et al. 2019). Oils and lipid

✉ Achmad Qodim Syafaatullah
Achmadqodims@atim.ac.id

[1] Department of Mineral-Chemical Engineering, Politeknik ATI Makassar, Jl. Sunu No.220, Kota Makassar 90211, Indonesia

components can be recovered well using organic solvents like methylene chloride and n-hexane, although they are hazardous. Additionally, traditional approaches are typically expensive and time-consuming (Kusuma and Mahfud 2017; Megawati et al. 2019). The shortcomings of these conventional techniques highlight the necessity of utilizing cutting-edge extraction technologies like microwave-assisted hydrodistillation (MAHD).

MAHD techniques will be highly effective, affordable, low-cost, ecologically benign, and able to produce high-quality products of *Citrus hystrix leaf* essential oil (Sopi et al. 2021). MAHD causes the plant's glandular and vascular systems to heat water molecules during the essential oil extraction process selectively. This causes the temperature to rise quickly, frequently above the boiling point of water, which ruptures cell walls and releases essential oils into the surrounding medium (Quyen et al. 2020). Solid material-to-liquid solvent (F/S) ratio, extraction duration, and microwave power are some of the factors that influence extraction efficiency in the MAHD process. The extraction efficiency is directly impacted by these factors, which also interact with one another (Nurhadi et al. 2022). In addition, the response surface methodology (RSM) was used to examine the effects of extraction duration, microwave irradiation power, and water volume to plant mass ratio on the extraction yield of *Citrus hystrix* leaves under the microwave-assisted hydrodistillation method.

RSM uses statistical methods to characterize a desired response or an outcome of interest about a set of process factors (Rusydan et al. 2021). RSM has many advantages, including easily accessible, effective, and simple experimental designs for the technique (Mas'Ud et al. 2017). Additionally, RSM may handle problems with both linear and nonlinear multivariate regression and cut down on the number of experiment trials. Optimization of essential oil extraction yield from *Citrus hystrix* leaves in this study was carried out using Box-Behnken design (BBD) and face-centered central composite design (FCCCD) using software design experts. The value of the extraction rate constant must be determined by running several models, including the first-order model, second-order model, Peleg model, power law model, and parabolic diffusion model, to support the potential of the scale-up process (Karabegoić et al. 2023)–(Maharaj and McGaw 2020).

2 Materials and methods

2.1 Materials

The materials used in this research were *Citrus hystrix* leaves from Makassar, South Sulawesi, Indonesia. The leaves were harvested and washed to remove the impurities on the leaves. After that, they were chopped into small pieces, approximately 0.5 mm, to improve the contact area between the leaves and the solvent during the extraction process (Ngan et al. 2019).

2.2 Microwave-assisted hydrodistillation

In this investigation, 600 mL of H_2O was utilized as the solvent in a flask that was fastened directly to the condenser lid. A microwave (Sharp, 220 V, 50 Hz) helped with the extraction process by raising the temperature and distilling the essential oil extract. The extraction process was done over 3 h. The ratio of feed (*Citrus hystrix* leaves) to solvent was 0.35–0.45, and the power of the microwave was 270–630 W. The yield of essential oils from *Citrus hystrix* leaves was calculated by

$$Yield(\%) = \frac{the\ weight\ of\ essential\ oils}{thevweight\ ofvCytrus\ hystrix\ leaves} \times 100\% \quad (1)$$

The scheme of the extraction process can be seen in Fig. 1. Since the extraction efficiency is highly temperature-dependent, the MAHD process was carried out under controlled thermal conditions. Microwave power and extraction time were adjusted to regulate heating, while water served as a natural buffer to prevent overheating. The temperature was continuously monitored during the extraction, ensuring that the process remained within safe limits and the essential oil quality was preserved. The yield of essential oils was determined gravimetrically, expressed as the ratio between the weight of essential oils obtained and the weight of *Citrus hystrix* leaves (Eq. 1). This gravimetric approach is commonly applied in essential oil research, as it directly reflects the extraction efficiency of the process. Gas chromatography-mass spectrometry (GC–MS) analysis was subsequently employed to characterize the chemical composition and relative abundance of volatile constituents. While GC–MS provides detailed information on compound identification and relative percentage, the overall extraction yield was considered more accurately represented by gravimetric calculation rather than compound quantification through internal standard methods.

2.3 Optimization RSM model

The experimental data of yield was analyzed to determine the optimum condition of the process using RSM via Design Expert 13 software. The development model was analyzed to obtain equations that represent experimental research. The FCCCD and BBD were used to analyze the research data. The independent variables of the experimental design can be seen in Table 1, with yield as a response parameter. This RSM method was used to minimize the number of variables and predict the optimum condition variables (Syafaatullah et al. 2023).

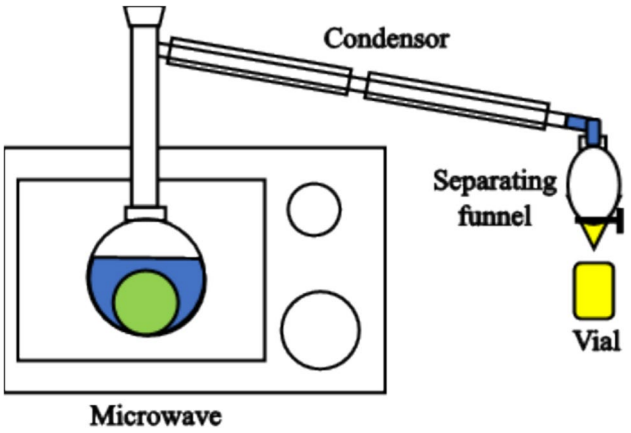


Fig. 1 Microwave-assisted hydrodistillation (MAHD) process diagram for essential oil extraction from *Citrus hystrix* leaves

Table 1 Design of experiment

Factor	Unit	Low	High
Power	Watt	270	630
F/S ratio	g/ml	0.35	0.45
Time extraction	Minutes	30	150

2.4 Kinetic analysis

The impact of the experimental parameters (microwave power, F/S ratio, and extraction duration) on yield was examined. There are three steps in the extraction process mechanism. First, the components are mixed, and the solvent that results dissolves the essential oils by penetrating the particles. The dissolved essential oils then spread throughout the material's surface through an internal diffusion mechanism. The essential oils then disperse and enter the solution's main body (external diffusion) (Wang et al. 2023).

2.4.1 First-order model

The first-order model represents essential oils that are treated as pseudo-components with insignificant changes in composition during the extraction process. There are no chemical reactions during the process. The process of extraction occurs in batch processes (Haqqyana et al. 2022). The mass transfer rate model can be expressed in differential form:

$$\frac{dC_t}{dt} = k_1(C_s - C_t) \tag{2}$$

$$ln\left[\frac{C_s}{C_s - C_t}\right] = k_1 t \tag{3}$$

$$log\left[C_s - C_t\right] = -\frac{k_1}{2.303}t + log\left[C_s\right] \tag{4}$$

Equation 4 was plotted between log (*Cs*-*Ct*) and *t* to determine the slope and intercept of the linear equation. The results of the slope and intercept of the linear equation were used to define the values of k_1 and *Cs*. The value of k_1 was related to the first-order constant rate, and the value of *Cs* was related to the maximum capacity of extraction.

2.4.2 Second-order model

The second-order kinetic model assumes that essential oil compounds are located on the surface of the material particles, so the solvent quickly dissolves the compounds of essential oils at the beginning of the extraction process. Then, the extraction of essential oils remaining in the damaged particles is controlled by unhindered slow diffusion. The diffusion process of essential oil compounds that are stored in unbroken particle cells occurs very slowly (Dulo et al. 2023). The mathematical equation of the second-order kinetics can be shown in Eq. 5.

$$\frac{dC_t}{dt} = k_1(C_s - C_t)^2 \tag{5}$$

$$C_t = \frac{C_s^2 k_2 t}{1 + C_s k_2 t} \tag{6}$$

$$\frac{t}{C_t} = \frac{t}{C_s} + \frac{1}{k_2 Cs^2} \tag{7}$$

Plotting *t*/*Ct* against *t* reveals that Eq. 7 is a second-order linear equation. To find the values of k_2 and *Cs*, the slope and intercept are computed. The value of *Cs* was associated with the extract's maximal capacity, whereas the value of k_2 was associated with the second-order constant rate. Since the value of *h* represents the beginning rate of the extraction process at $t = 0$, it may be expressed as $k_2 Cs^2$. One definition of Eq. 7 is

$$\frac{t}{C_t} = \frac{t}{C_s} + \frac{1}{h} \tag{8}$$

2.4.3 Peleg model

The Peleg model is a hyperbolic-kinetic model that is applied to represent the extraction mechanism of biological compounds. There are two stages, which are assumed by the Peleg model. In the initial stage, the kinetic model

follows a first-order model mechanism, and in the next stage of the process, it decreases to zero-order (Das et al. 2021).

$$\frac{1}{Ct} = \frac{K_1}{t} + K_2 \tag{9}$$

Equation 9 was plotted between $\frac{1}{Ct}$ and $\frac{1}{t}$ to determine the slope and intercept of the linear equation. The results of the slope and intercept of the linear equation were used to define the value of K_1 and K_2. The value of K_1 was related to the Peleg-rate constant, and the value of K_2 was related to the Peleg capacity constant.

2.4.4 Power law model

The power law model is used to determine the extraction components by compound diffusion via non-swelling devices (Natolino and Porto Apr. 2020). The mathematical model is expressed in Eq. 10.

$$Ct = Bt^n \tag{10}$$

Table 2 Box-behnken design (BBD) in actual and prediction

Run	Power	Ratio F/S	Time extraction	Yield actual (%)	Yield prediction (%)	Error (%)
1	450	0.45	150	0.964519	0.901	0.063519
2	270	0.45	90	0.417	0.421	−0.004
3	630	0.35	90	1.23976	1.236	0.00376
4	630	0.45	90	0.862296	0.897	−0.0347
5	270	0.4	150	0.703833	0.764	−0.06017
6	450	0.4	90	0.904	0.904	0
7	450	0.45	30	0.264259	0.29	−0.02574
8	630	0.4	30	0.635875	0.576	0.059875
9	450	0.4	90	0.914	0.904	0.01
10	270	0.4	30	0	0.0492	−0.0492
11	630	0.4	150	1.12921	1.158	−0.02879
12	450	0.35	150	1.31871	0.981	0.33771
13	270	0.35	90	0.74619	0.712	0.03419
14	450	0.35	30	0.465286	0.529	−0.06371
15	450	0.4	90	0.894	0.904	−0.01

Table 3 Face-centered central composite design (FCCCD) in actual and prediction

Run	Power	Ratio F/S	Time extraction	Yield actual (%)	Yield prediction (%)	Error (%)
1	270	0.35	30	0	0.024	−0.024
2	450	0.4	150	1.09654	1.054	0.04254
3	450	0.4	90	0.904	0.902	0.002
4	270	0.4	90	0.542333	0.524	0.018333
5	270	0.35	150	0.955952	0.958	−0.00205
6	630	0.35	30	0.74119	0.711	0.03019
7	450	0.35	90	1.10838	1.078	0.03038
8	450	0.4	90	0.914	0.902	0.012
9	630	0.35	150	1.38981	1.426	−0.03619
10	630	0.45	30	0.535667	0.533	0.002667
11	630	0.45	150	0.952481	0.928	0.024481
12	450	0.4	90	0.894	0.902	−0.008
13	630	0.4	90	1.02079	1.043	−0.02221
14	450	0.45	90	0.764333	0.799	−0.03467
15	450	0.4	30	0.343625	0.39	−0.04638
16	270	0.45	30	0	0.405	−0.405
17	270	0.45	150	0.548444	0.578	−0.02956

where Ct is the value of yield essential oils at a specific time t (min), n is the power law exponent (< 1), and B is related to the extraction rate constant.

2.4.5 Parabolic diffusion model

The parabolic diffusion model is similar to the Peleg model, in which the equation model assumes a two-step extraction mechanism, an initial and rapid dissolution step for essential oil compounds on the particle surface, followed by diffusion through the particle (Raji and Kiani 2020). The mathematical model can be expressed as

$$Ct = A_0 + A_1 t^{\frac{1}{2}}$$

where Ct is the value of yield essential oils at a specific time t (min), A_0 is related to the dissolution coefficient, and A_1 is related to the diffusion rate constant on the parameter of the parabolic diffusion model.

2.4.6 Statistical analysis

The validation of each order model is evaluated by the determinant coefficient (R^2) and root mean square error (RSME). The determinant coefficient (R^2) and RSME can be calculated as follows:

$$R^2 = 1 - \frac{\sum_{i=1}^{n} \left(X_i - \hat{X}_i \right)^2}{\sum_{i=1}^{n} \left(X_i - \hat{X} \right)^2} \quad (11)$$

$$RSME = \sqrt{\frac{1}{n} \sum_{i=1}^{n} \left(X_i - \hat{X}_i \right)^2} \quad (12)$$

where.
x_i = value of the yield extract experiment.
$\hat{x}_i$ = value of the yield extract predicted.
$\hat{x}$ = value of the yield extract mean.

2.5 Fourier transformed infrared spectroscopy (FTIR)

The functional groups of essential oils were analyzed by FTIR with the specification "Thermo Scientific Nicolet iS10." The results of FTIR analysis were % transmittance between wavenumber of 500 and 4000 cm^{-1} (Sopi et al. 2021). The match of the component was shown in the results, too.

2.6 Gas chromatography-mass spectrometry

The chemical components of essential oils were analyzed by GC–MS with the specification "Thermo Scientific Trace 1310 ISQ LT Single Quadrupole GC–MS." The relative amount of each component was calculated based on the GC peak area (Quyen et al. 2020). Before analysis, the EO samples were diluted 1:100 (v/v) in n-hexane, filtered through a 0.45 µm PTFE membrane, and 1 µL was injected in split mode (10:1) onto a DB-5MS column using helium as the carrier gas. Compound identification was carried out by comparison with NIST/Wiley libraries and confirmed with Kováts retention indices. The

Table 4 ANOVA of each model based on the response variables

RSM design	Responses	Mean	Std. dev	CV %	R^2	Adjusted R^2	Predicted R^2
BBD	Yield (%)	0.7639	0.0645	8.45	0.9887	0.9683	0.8204
FCCCD	Yield (%)	0.7477	0.0425	5.68	0.9945	0.9875	0.9299

Table 5 Mathematical equation of each model RSM

RSM design	Response variable	Mathematic equation
BBD	Yield (%)	$0.579164 + 0.005470\ X_1 - 9.12688\ X_2 + 0.021777\ X_3 - 0.001341\ X_1X_2 - 4.87269.10^{-6}\ X_1X_3 - 0.012764\ X_2X_3 - 3.45144.10^{-6}\ X_1^2 - 9.65549\ X_2^2 - 0.000049\ X_3^2$
FCCCD	Yield (%)	$0.307677 + 0.006492\ X_1 - 10.59230\ X_2 + 0.027469\ X_3 - 0.003269\ X_1X_2 - 5.08059.10^{-6}\ X_1X_3 - 0.026638\ X_2X_3 - 3.65186.10^{-6}\ X_1^2 + 14.58975\ X_2^2 - 0.000050\ X_3^2$

X_1, power (W); X_2, F/S ratio (g/ml); X_3, time (minutes)

Table 6 ANOVA and regression coefficient of each RSM model

RSM design	Source	Sum of squares	*df*	Mean square	*F*-value	*p*-value
BBD	Model	1.82	9	0.2021	48.52	0.0002
	X_1-Power	0.5001	1	0.5001	120.05	0.0001
	X_2-F/S ratio	0.1990	1	0.1990	47.78	0.0010
	X_3-Time extraction	0.9459	1	0.9459	227.08	< 0.0001
	X_1X_2	0.0006	1	0.0006	0.1399	0.7237
	X_1X_3	0.0111	1	0.0111	2.66	0.1639
	X_2X_3	0.0059	1	0.0059	1.41	0.2887
	X_1^2	0.0462	1	0.0462	11.08	0.0208
	X_2^2	0.0022	1	0.0022	0.5165	0.5045
	X_3^2	0.1130	1	0.1130	27.13	0.0034
	Residual	0.0208	5	0.0042		
	Lack of fit	0.0206	3	0.0069	68.76	0.0144
	Pure of error	0.0002	2	0.0001		
FCCCD	Model	2.29	9	0.2548	141.12	< 0.0001
	X_1-Power	0.6725	1	0.6725	372.42	< 0.0001
	X_2-F/S ratio	0.1944	1	0.1944	107.68	< 0.0001
	X_3-Time extraction	1.10	1	1.10	611.45	< 0.0001
	X_1X_2	0.0069	1	0.0069	3.83	0.0911
	X_1X_3	0.0241	1	0.0241	13.34	0.0082
	X_2X_3	0.0511	1	0.0511	28.29	0.0011
	X_1^2	0.0375	1	0.0375	20.77	0.0026
	X_2^2	0.0036	1	0.0036	1.97	0.2028
	X_3^2	0.0866	1	0.0866	47.97	0.0002
	Residual	0.0126	7	0.0018		
	Lack of fit	0.0206	5	0.0025	24.88	0.0391
	Pure of error	0.0002	2	0.0001		

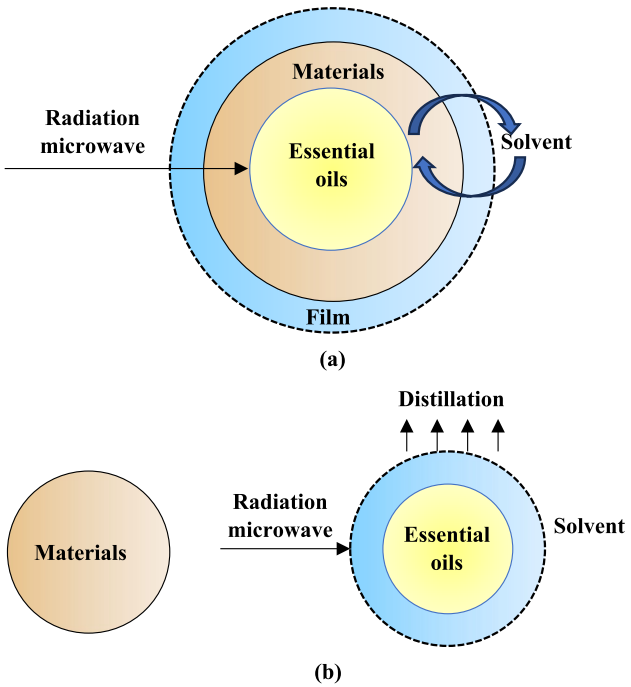


Fig. 2 Mass transfer mechanism of essential oils during microwave-hydrodistillation: **a** extraction process and **b** distillation process

identification of volatile compounds was performed by comparing the obtained mass spectra with reference spectra from the NIST 14 and Wiley 275 mass spectral libraries. To increase reliability, compound identification was further supported by calculating Kováts retention indices (RI) using a homologous series of n-alkanes (C8–C20) analyzed under identical conditions. Only compounds with a match quality above 85% in the database and consistent RI values with literature data were considered correctly identified.

2.7 Scanning electron microscopy (SEM)

Scanning electron microscopy was used to analyze the morphology of the samples. The samples were ground into powder before analyzing SEM. Powder samples of before and after extract were coated with carbon tape and analyzed with SEM (Hitachi Flexsem 1000) at 8000 × magnification with the high vacuum method (Nurhadi et al. 2022).

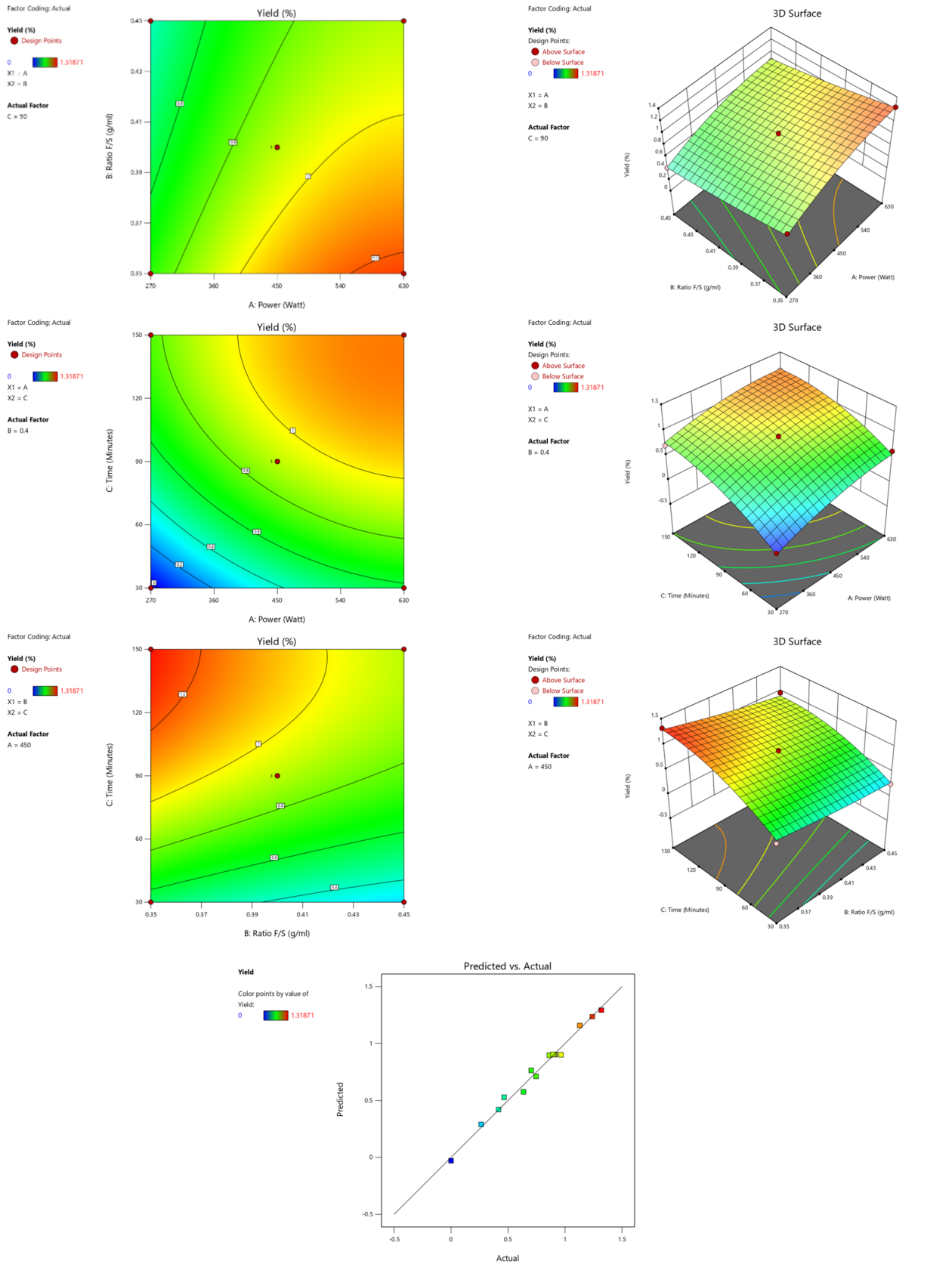


Fig. 3 Contour and 3D surface plots of **a** power and F/S ratio, **b** power and extraction time, **c** F/S ratio and extraction time, and **d** comparison of predicted and actual yield based on the BBD model

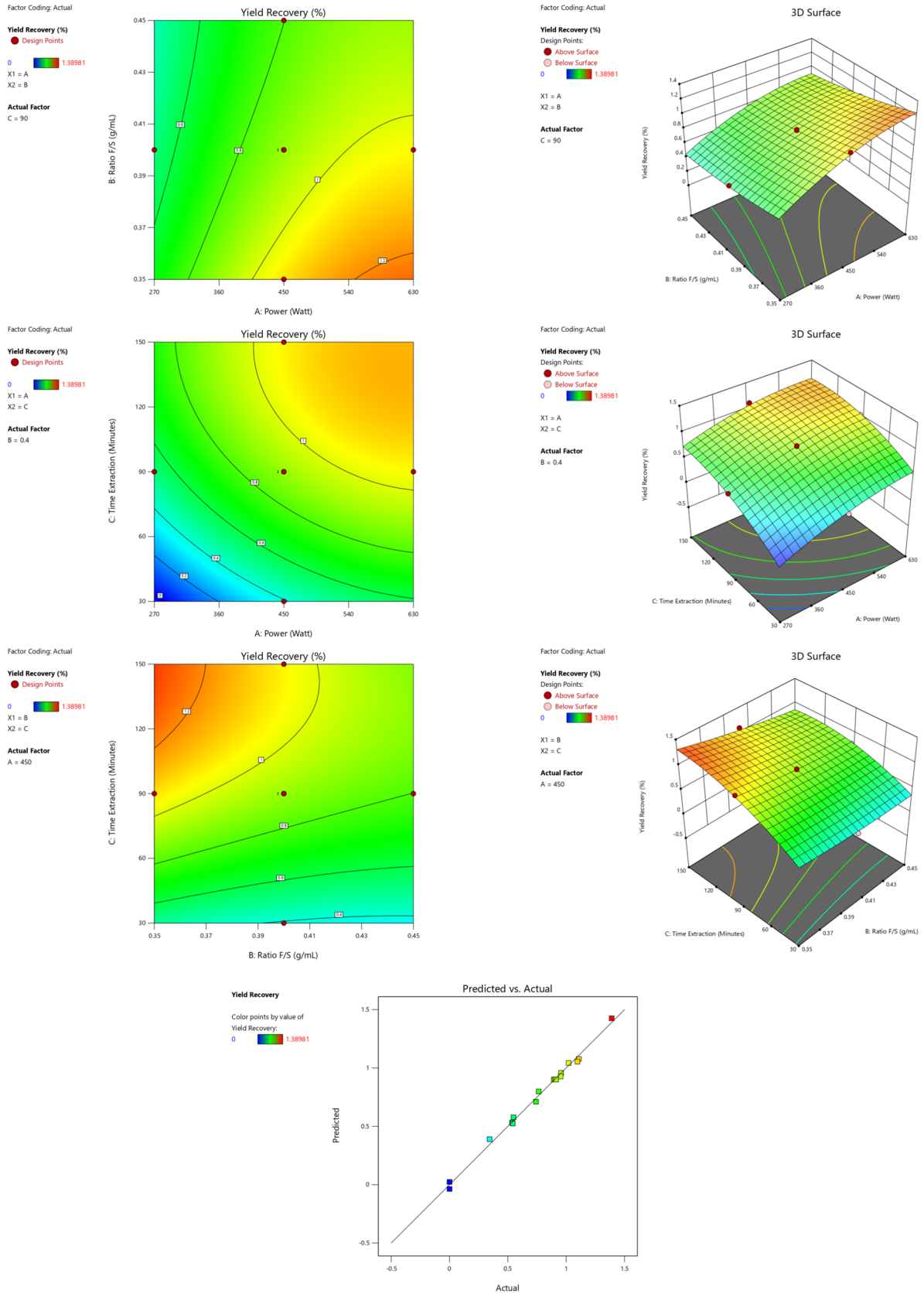


Fig. 4 Contour and 3D surface plots of **a** power and F/S ratio, **b** power and extraction time, **c** F/S ratio and extraction time, and **d** comparison of predicted and actual yield based on FCCCD model

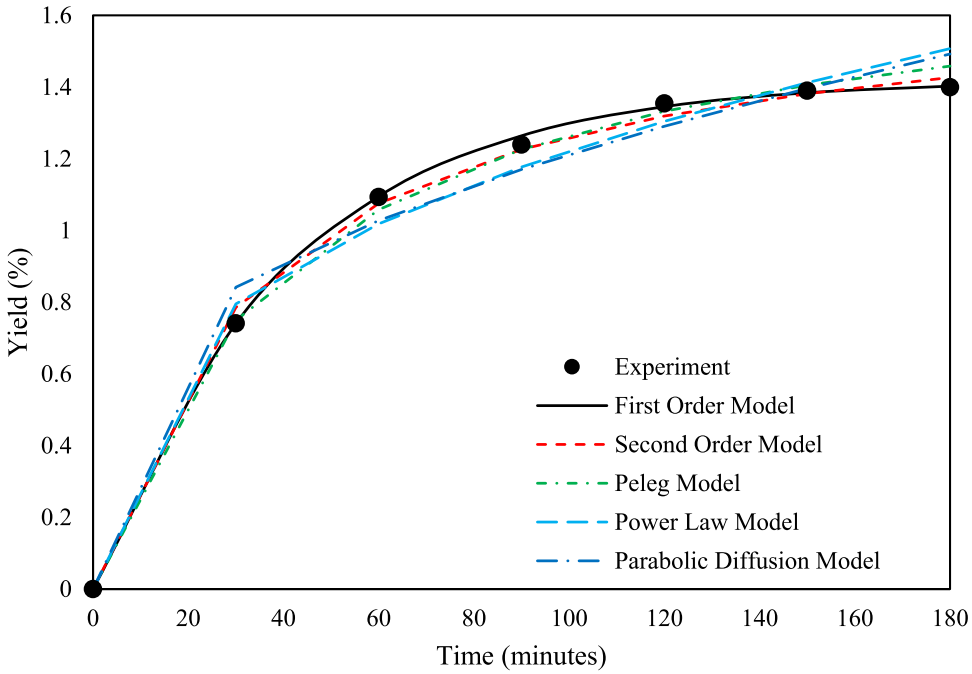


Fig. 5 Comparison of each kinetics model on power of 630 watts and F/S ratio of 0.35

3 Results and discussion

3.1 The RSM results

In this study of *Citrus hystrix* leaves extraction using the MAHD technique, the BBD and FCCCD were used. In this study, 32 trials for both BBD and FCCCD designs were carried out. Design-Expert 13 software was used to analyze the data, and the 2nd-order polynomial model was modified as follows:

$$Y = \beta_0 + \beta_1 x_1 + \beta_2 x_2 + \beta_3 x_3 + \beta_{12} x_1 x_2 + \beta_{13} x_1 x_3 + \beta_{23} x_2 x_3 + \beta_{11} x_1^2 + \beta_{22} x_2^2 + \beta_{33} x_3^2$$

where Y is the yield of the mathematical model. The values x_1, x_2, and x_3 indicate the independent variables: the power (W), the F/S ratio (g/ml), and the extraction time (min). Table 2 shows that the extraction yield varied between 0.26 and 1.32%, with predicted values showing close agreement with the experimental results, and Table 3 shows that the extraction yield ranged from 0.34 to 1.39%, with predicted values closely matching the experimental data. The small error values (–0.046 to + 0.043%) indicate that the model reliably represents the extraction process. The small errors (–0.06 to + 0.34%) indicate that the model accurately represents the extraction process. A mathematical model of each design can be seen in Table 5. Based on ANOVA results in Table 4, the R^2 value of each model (0.95–0.99) is close to 1, indicating that each model can represent the actual experiment. The difference between adjusted R^2 and predicted R^2 is less than 0.2, indicating that the predicted R^2 is in good agreement with the adjusted R^2. It means both of the models show mathematical equations that have good predictive ability (Rusydan et al. 2021). Standard deviation indicates the degree of data spread on the result parameters, while mean displays the average value of the resulting response parameters in Table 4. The data dispersion in relation to the average value is small when the standard deviation value is small. The RSM model does not significantly interpret the intercepted value, the sign that appears before any mathematical equations (Table 5) (Mas'Ud et al. 2017).

The quadratic model's yield response parameter for both the BBD and FCCCD designs has a p-value < 0.05 for the analysis of variance (ANOVA) (Table 6). This indicates that the model is logical, valid, and significant, with p-value yield parameters of 0.0002 and < 0.0001 for BBD and FCCCD, respectively (Karabegoić et al. 2023). The independent variables (X_1, X_2, and X_3) in Table 4 have a value of less than 0.05, which indicates that these parameters have a significant effect on the yield parameter (Didar and Hesarinejad 2022).

The mass transfer mechanism of essential oils during microwave-hydrodistillation is illustrated in Fig. 2. In the extraction stage (Fig. 2a), microwave radiation penetrates the plant matrix, leading to cell wall disruption and facilitating the release of essential oils into the surrounding solvent. This interaction promotes diffusion and enhances the mobility of volatile compounds within the film structure. In the subsequent distillation stage (Fig. 2b), continuous microwave irradiation supports the volatilization of essential oils, which are carried away by the solvent vapor. The vapor phase is

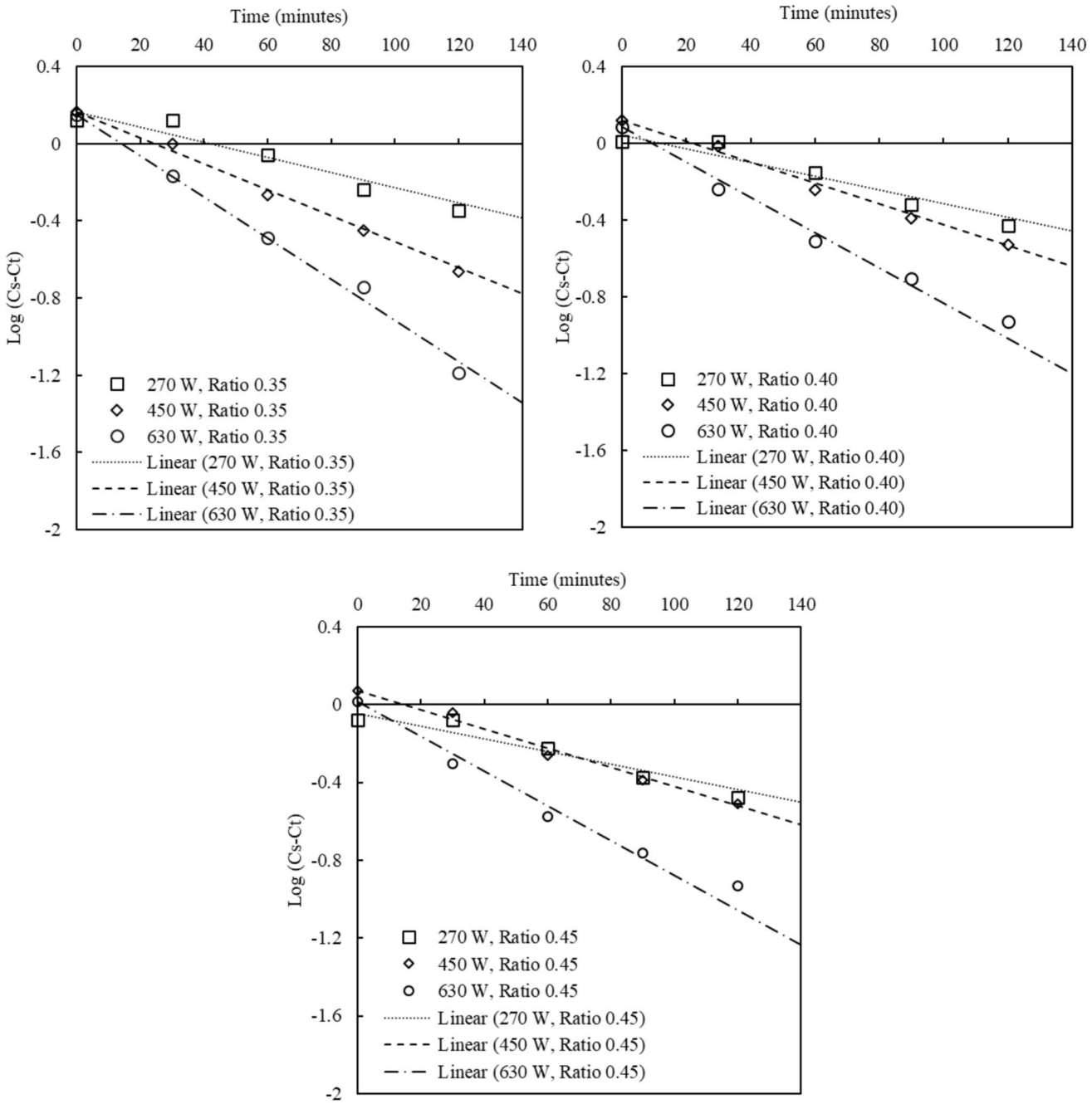


Fig. 6 Kinetics of the first-order model for each F/S ratio

Table 7 The optimum condition of each model RSM

RSM design	Optimal condition			Yield predicted (%)	Yield actual (%)	Residual (%)
	Power (W)	F/S ratio (g/ml)	Time (minutes)			
BBD	630.000	0.35	135.788	1.367	1.37851	0.01151
FCCCD	630.000	0.35	150.000	1.426	1.38981	−0.03619

then condensed, resulting in the separation and recovery of essential oils with improved efficiency (Maharaj and McGaw 2020). The effect of microwave power (W) is significant on the yield extract, which is shown by the BBD and FCCCD plots in Figs. 3 and 4, and is proven by the high *F*-value (120.05 and 372.42, respectively). In both Figs. 4 and 5, it shows that increasing yield is related to increasing power. Increasing yield is caused by increasing power; the temperature increase produced by the MAHD process is faster. Increasing temperature is caused by the microwave emission mechanism. The injected microwaves will penetrate the *Citrus hystrix* leaves sample, which has a dipole electric. This means that the molecule has two charges: negative on one side and positive on the other. The electromagnetic energy emitted will be absorbed by these molecules. The changing electric field due to microwave penetration will make these molecules spin and rotate. The rotation of the molecules will produce friction, which results in heat on the sample surface. This mechanism will increase the temperature of the sample and solvent. In contrast, when temperatures increase, surface tension decreases, which can damage the cell walls of the material. This rupture will change the morphological structure of the sample, as shown in Fig. 6. Microwave heating is carried out directly into the material so that the desired heat by the material is achieved more quickly compared to conventional heating. The kinetic energy of the solvent's particles will rise with temperature, which will accelerate the solvent's diffusion into the substance. As the temperature rises, the diffusivity value increases proportionately. Apart from that, kinetic energy also causes good dissociation to release volatile compounds from the material. This mechanism will continue until it reaches equilibrium. Therefore, it can be concluded that as power increases, so will the temperature and the amount of essential oils produced (Letchumanan et al. Dec. 2023; Athanasiadis et al. 2023; Messadi et al. 2023).

The high *F*-value and low *p*-value in Table 6 indicate that the F/S ratio in Figs. 3 and 4 affects yield. The solvent's ability to extract the substance is correlated with the F/S ratio. As can be seen from Figs. 1 and 2, the yield extract will decrease as the F/S ratio increases. The contact area between the materials and the solvent, as well as the mass transfer and solvent diffusion, all rise as the F/S ratio increases. The diffusion rate may therefore be accelerated by this process. On the other hand, lowering the F/S ratio will boost the solvent's extraction ability and yield as well (Wang et al. 2023). In addition, the bottom and upper limits were used to prevent burnt materials when the solvent is completely evaporated during the process. Determining the optimum conditions for the F/S ratio is needed to minimize production costs when carried out on a large scale (Phat et al. 2022).

The yield extraction increased as the extraction duration increased under different combinations of microwave power (W) and F/S ratio (g/ml) (Figs. 3 and 4). The yield increased linearly from the start of extraction to the 60-min mark. Despite the lack of a linear increase, the yield increased from 60 to 120 min before progressively declining. After more extraction time, saturation equilibrium will be reached in terms of both the material's internal and external concentrations. The extraction yield is likely to plateau in an equilibrium state. The yields were 1.39% and 1.40% (630 W, F/S ratio 0.35), respectively, at 120 and 150 min in this investigation. Diffusion from solute to solvent is not occurring at this moment (Wang et al. 2023; Raji and Kiani 2020; Mahfud et al. 2020). In another study, the extraction of essential oils from *Citrus microcarpa* using the hydrodistillation method had an insignificant increase after 60 min. In this condition, equilibrium has occurred, so that there is no significant change in the yield produced (Phat et al. 2022). Degradation of bioactive compounds occurs at a long extraction time of the MAHD process, to which the materials will be exposed to excess microwave radiation (Murni et al. Dec. 2021).

As shown in Table 7, the optimal conditions considered for BBD design involve power microwave of 630 W, F/S ratio of 0.35, and extraction time of 135.788 min. At optimal conditions, consider that the FCCCD design has similar conditions, except for an extraction time of 150 min. The maximum predictive yield is estimated, and the values are 1.367% (BBD) and 1.426% (FCCCD). Meanwhile, the residual values between the actual and predicted values are 0.01151% and − 0.03619% (FCCCD). The residual value is smaller than 3%, which indicates that there is conformity between the predicted results and the actual results. Both designs show the same conclusion, namely optimal conditions for a power of 630 W and a ratio of 0.35.

3.2 Kinetics modeling analysis

This study used the first-order, second-order, Peleg, power law, and parabolic diffusion models of kinetics. The extraction mechanism under different conditions is described using a kinetics analysis model. In order to track changes in the response variable to the MAHD process from 0 to 180 min, kinetic analysis was carried out under the ideal conditions (630 W, F/S ratio 0.35), as detailed in Table 7. The first-order kinetics model is predicated on a number of assumptions. Initially, the substance contains a consistent solute of essential oils. Second, essential oils are found within the material rather than on its surface. Third, size, shape, and essential quantity are considered to be in an isotropic state (Phat et al. 2022). The first-order kinetics model is used in Eq. 4, and the results are shown in Table 8. When the power of the microwave is increasing, the value of k_1 is increasing too. High power causes an increased diffusion rate, which is related to the constant value of the extraction rate (Letchumanan et al. Dec. 2023). By contrast, the value of k_1 rises when the F/S

Table 8 Kinetics extraction and statistical parameters of first-order model

Model equation	*P* (W)	F/S ratio (g/ml)	Model parameters		Statistical parameters	
			k_1	*Cs*	R^2	RSME
First-order model	270	0.35	0.0084	1.3276	0.9707	0.1171
		0.40	0.0077	1.0224	0.9619	0.0848
		0.45	0.0070	0.8375	0.9595	0.0644
	450	0.35	0.0155	1.4637	0.9958	0.0333
		0.40	0.0125	1.3130	0.9920	0.0325
		0.45	0.0133	1.1727	0.9911	0.0333
	630	0.35	0.0246	1.4198	0.9899	0.0102
		0.40	0.0211	1.2187	0.9624	0.0299
		0.45	0.0206	1.0340	0.9468	0.0945
Mean					0.9745	0.0556

Table 9 Kinetics extraction and statistical parameters of second-order model

Model equation	*P* (W)	F/S ratio (g/ml)	Model parameters			Statistical parameters	
			k_2	*h*	*Cs*	R^2	RSME
Second-order model	270	0.35	0.0019	0.0106	2.3779	0.8074	0.1128
		0.40	0.0018	0.0073	1.9847	0.7023	0.0807
		0.45	0.0018	0.0054	1.7184	0.6306	0.0613
	450	0.35	0.0053	0.0236	2.1180	0.9635	0.0467
		0.40	0.0039	0.0163	2.0465	0.9318	0.0424
		0.45	0.0030	0.0123	2.0199	0.8574	0.0440
	630	0.35	0.0167	0.0486	1.7049	0.9966	0.0254
		0.40	0.0188	0.0390	1.4408	0.9997	0.0075
		0.45	0.0218	0.0325	1.2207	0.9991	0.0094
Mean						0.8765	0.0478

ratio falls. Similar circumstances also apply to the *Cs* value or maximum extraction capacity. It correlates with surface contacts; maximizing the surface area of materials is impacted by lowering the F/S ratio (Wang et al. 2023).

The second-order kinetics model used Eq. 7, and the results can be seen in Table 9. It can be implied that the second-order kinetics model is more suitable at high microwave radiation power. It shows that the value of the determinant coefficient is close to 1, and the value of the RSME is close to 0. The second-order kinetics model assumes that there is a significant rate of extraction at the initial extraction. It occurs because the high power of the microwave has more energy to raise the temperature quickly, which affects the diffusion mechanism. It implies that there is an additional driving force in the mass transport process using microwaves, which is different from conventional heating extraction mechanisms (Haqqyana et al. 2022). Different kinetics models, such as the parabolic diffusion model, power law, and Peleg, are used to compare and explain the importance of the F/S ratio and microwave radiation. Other studies claim that the Peleg model was used to evaluate the yield and extraction rate of pectin and phenol compounds at equilibrium at different parameters (Das et al. 2021). The Peleg model performed well in fitting the research data on essential oil extraction utilizing the MAHD procedure (Table 10). RSME was 0.595, and R^2 was 0.9802, according to the implication (Wang et al. 2023).

Meanwhile, the behavior of H_2O as a solvent for essential oil extraction utilizing the MAHD process is described by constant parameter B of the power law model. The high microwave power has an impact on raising the value of the B parameter, as Table 11 illustrates. A high value of B is achieved for low F/S ratios, just like in previous kinetics models. Water's capacity to transport and absorb microwave thermal radiation damages cell walls, as shown by the B parameter's value. The diffusional exponent value n ($n < 1$) indicates the transport mechanism in the MAHD process during the diffusion and washing stages. An easier solute transport during the stage process is indicated by a smaller value of n. The washing stage means the extraction

Table 10 Kinetics extraction and statistical parameters of Peleg model

Model equation	P (W)	F/S ratio (g/ml)	Model parameters				Statistical parameters	
			K_1	Extraction rate $= 1/K_1$	K_2	$Cs = 1/K_2$	R^2	RSME
Peleg model	270	0.35	109.0.628	0.0092	0.2857	3.5006	0.9547	0.1098
		0.40	161.9696	0.0062	0.2879	3.4737	0.9491	0.0806
		0.45	219.1315	0.0046	0.2886	3.4645	0.9493	0.0624
	450	0.35	51.4473	0.0194	0.3707	2.6977	0.9979	0.0194
		0.40	74.0427	0.0135	0.3438	2.9090	0.9992	0.0804
		0.45	100.8340	0.0099	0.2738	3.6518	0.9982	0.0919
	630	0.35	23.3488	0.0428	0.5559	1.7987	0.9848	0.0428
		0.40	26.3527	0.0379	0.6859	1.4580	0.9976	0.0379
		0.45	31.2927	0.0320	0.8122	1.2312	0.9910	0.0099
Mean							0.9802	0.0595

Table 11 Kinetics extraction and statistical parameters of power law model

Model equation	P (W)	F/S ratio (g/ml)	Model parameters		Statistical parameters	
			B	n	R^2	RSME
Power law model	270	0.35	0.0266	0.7165	0.9275	0.1252
		0.40	0.0157	0.7613	0.9216	0.0886
		0.45	0.0105	0.7914	0.9235	0.0669
	450	0.35	0.0711	0.5905	0.9268	0.1036
		0.40	0.0413	0.6642	0.9327	0.0877
		0.45	0.0261	0.7277	0.9284	0.0846
	630	0.35	0.2364	0.3567	0.9335	0.0696
		0.40	0.2064	0.3466	0.9621	0.0391
		0.45	0.1737	0.3472	0.9615	0.0324
Mean					0.9353	0.0775

Table 12 Kinetics extraction and statistical parameters of parabolic diffusion model

Model equation	P (W)	F/S ratio (g/ml)	Model parameters		Statistical parameters	
			A_0	A_1	R^2	RSME
Parabolic diffusion model	270	0.35	0.0000	0.0760	0.9941	0.1665
		0.40	0.0000	0.0557	0.9923	0.1240
		0.45	0.0000	0.0433	0.9912	0.0973
	450	0.35	0.3373	0.1107	0.9696	0.3421
		0.40	0.1671	0.1006	0.9932	0.2675
		0.45	0.0933	0.0914	0.9919	0.2355
	630	0.35	0.3929	0.0819	0.9009	0.0676
		0.40	0.3276	0.0682	0.9449	0.0410
		0.45	0.2746	0.0577	0.9469	0.0340
Mean					0.9694	0.1528

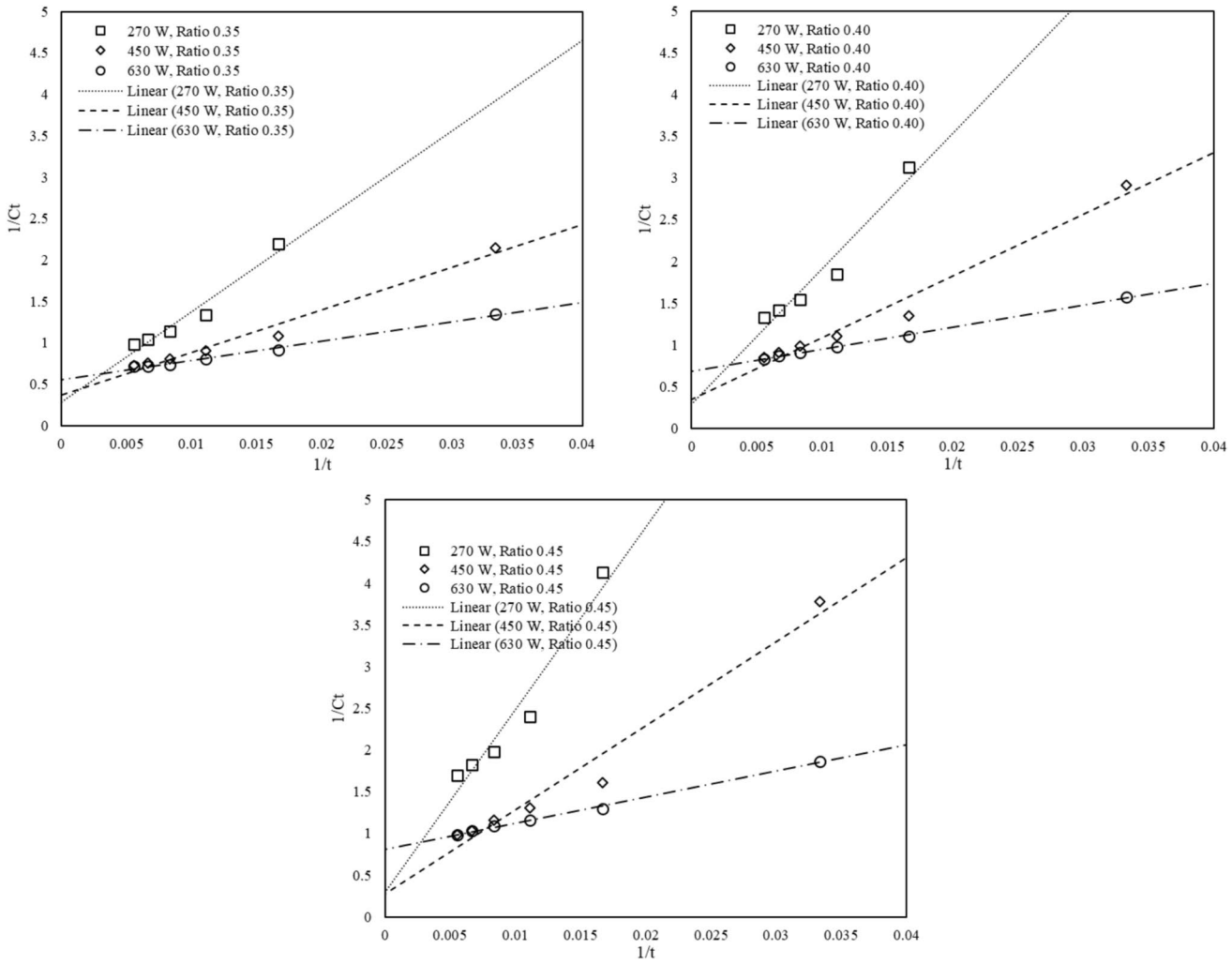


Fig. 7 Kinetics of the Peleg model for each F/S ratio

of essential oil volatile compounds, which are located on the surface matrix (Mahfud et al. 2020).

According to Table 12, the parabolic diffusion model has a low RSME (0.0410–0.1665) and a comparatively high R^2 (0.9–0.99). A_0 indicates that the dissolving coefficient is zero at 270 W. In this condition, the value of 0 indicates that there is no disintegration. Similar to a washing mechanism, a dissolution mechanism is the extraction of essential oils from a material's surface. On the other hand, the value of A_1 represents the diffusion mechanism of the second step of essential oil extraction. Similar to the power law concept, when the microwave's power rises and the F/S ratio falls, the values of A_0 and A_1 rise as well. The MAHD process of *Citrus hystrix* essential oil happens with a more intense dissolving mechanism than the diffusion mechanism at greater power, as indicated by the fact that $A_0 > A_1$ (Menkiti and Agu 2019). The models' best fit improved in the following order according to the determinant constant (R^2) and RSME values: the Peleg model, the first-order model, the parabolic diffusion model, the power law model, and the second-order model. Figure 5 displays a comparison of each model at 630 W and an F/S ratio of 0.35. Figures 6 and 7 display the two best kinetics models: the Peleg model and the first-order model. According to the statistical parameters, the first-order and Peleg models demonstrated the best fit compared to other models. This result indicates that the first-order model is more representative of describing the kinetics of essential oil extraction. In this study, the extraction of essential oil from kaffir lime leaves was better represented by the first-order kinetic model. This is because the essential oil components are distributed both on the surface and inside the plant matrix. During the MAHD process, microwave energy penetrates uniformly, causing simultaneous rupture of the cell walls and release of volatile compounds from both the external surface and the internal structure. Consequently, the

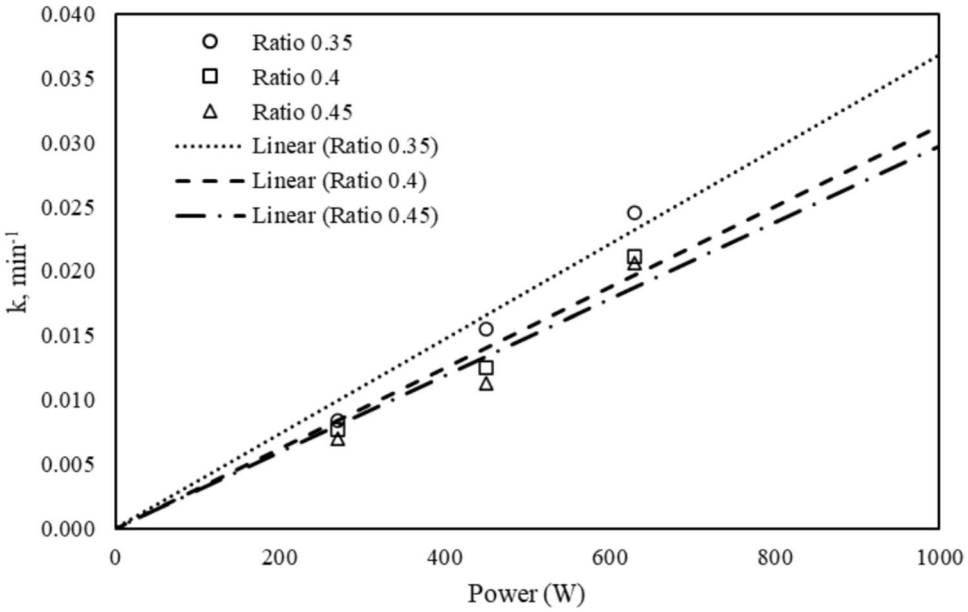


Fig. 8 The value of k for the first-order kinetic model

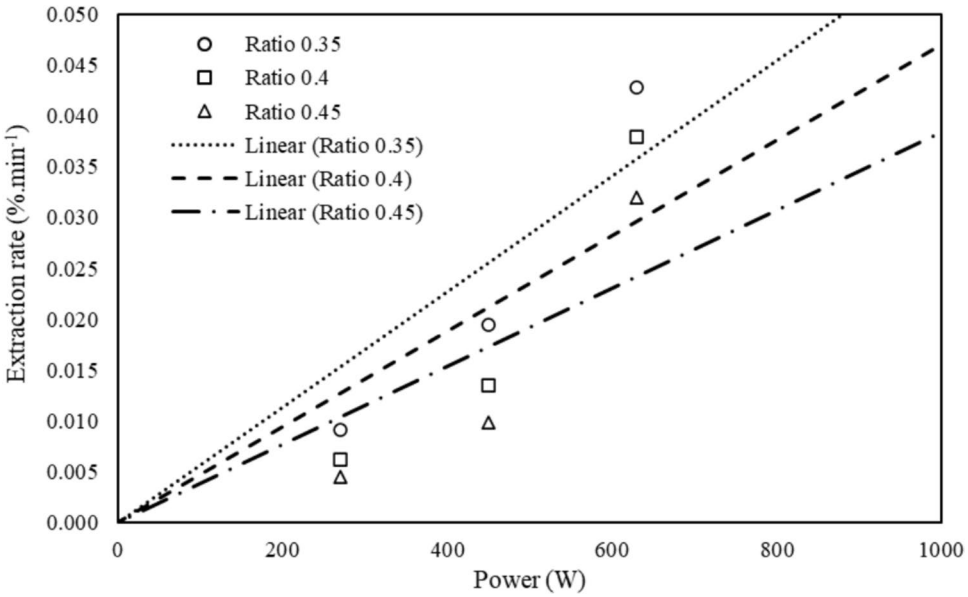


Fig. 9 The value of the extraction rate for the Peleg model

extraction behavior follows a homogeneous diffusion mechanism rather than a two-step process, making the first-order model more suitable to describe the kinetics of this system.

The regression of the extraction rate and k value at a broad range of power with each value of the F/S ratio is displayed in Figs. 8 and 9. The regression model, which is displayed in Table 13, uses mathematical regression to forecast the value of k and the extraction rate at any power. Table 13 indicates that the regression model outperforms the Peleg model in terms of first-order model predictability ($R^2 = 0.97–0.99$, RSME = 0.0013–0.0021). We conclude that the high-power microwave kinetic extraction model can be predicted using a first-order model.

3.3 FTIR, GC–MS, and SEM analysis

The FTIR spectrum of *Citrus hystrix* essential oil extract is presented in Fig. 10. Several characteristic absorption bands were observed that correspond to the major functional groups of citronellal. The band at 2914.40 cm^{-1} is assigned to C–H asymmetric stretching of CH_2 groups, while the band at 2712.85 cm^{-1} corresponds to aldehydic C–H stretching. A strong peak at 1724.35 cm^{-1} indicates the

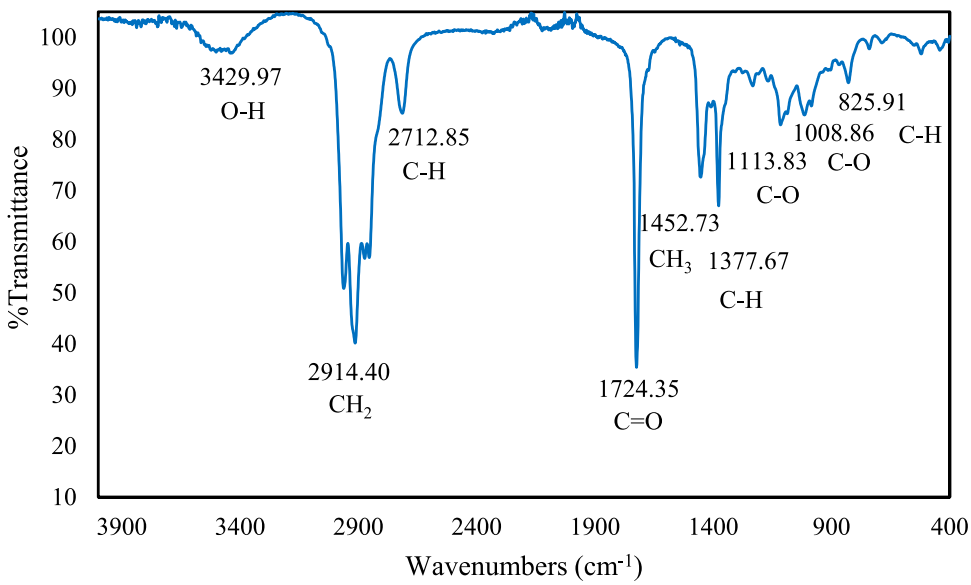


Fig. 10 FTIR analysis of essential oils from Citrus hystrix leaves

Table 13 First-order and Peleg model regression on each F/S ratio parameter

F/S ratio (g/ml)	First-order model	R^2	RSME	Peleg model	R^2	RSME
0.35	Y = 0.0000368X	0.9942	0.0013	Y = 0.0000568X	0.9455	0.0065
0.40	Y = 0.0000338X	0.9797	0.0018	Y = 0.0000471X	0.8974	0.0075
0.45	Y = 0.0000322X	0.9700	0.0021	Y = 0.0000384X	0.8701	0.0070

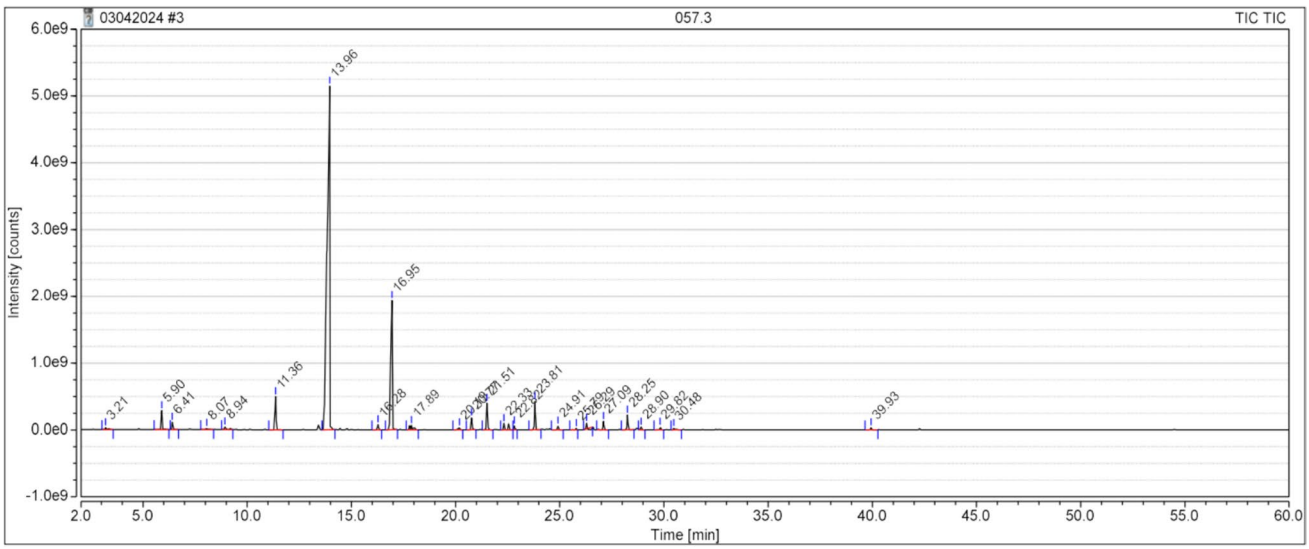


Fig. 11 GC-MS analysis of essential oils from Citrus hystrix leaves FTIR analysis of essential oils from *Citrus hystrix* leaves

presence of C = O stretching vibration of aldehyde groups, confirming the oxygenated nature of the extract. Additional bands at 1452.73 cm^{-1} and 1377.67 cm^{-1} are attributed to CH_3 asymmetric deformation of C–O–H groups, and the absorption at 1008.86 cm^{-1} represents C–O stretching vibration. These functional groups are characteristic of aldehydic monoterpenes such as citronellal (Lis et al. 2018; Songkro et al. 2012). These spectral features were compared with a reference library of standard compounds, and the software generated a similarity index. The essential oil extract exhibited a 93.69% match with citronellal, as presented in Table 14, confirming that the extract composition closely

Table 14 FTIR and match similarity compound analysis

Compound name	Match similarity (%)
Citronellal, 99%	93.69
2,6-Dimethyl-5-heptenal, tech., 80%	87.80
3-(Methylthio)butanal, 96%	83.43
2.3-Dimethylvaleraldehyde, 97%	79.69
Valeraldehyde, 97%	79.12
2-Methylvaleraldehyde, 98%	77.39
Nonylaldehyde, 98%	75.48
Heptaldehyde, 95%	75.45
8-Methyl-7-noneal, 98%	74.61

resembles that of citronellal. This result demonstrates that FTIR analysis not only identifies the functional groups but also quantifies the overall spectral similarity, thereby validating citronellal as the dominant constituent of *Citrus hystrix* essential oil (Prasetyaningrum et al. 2024).

Citrus hystrix essential oil leaves, which were extracted using the MAHD method, were analyzed by GC–MS to characterize the chemical composition of the essential oil extract (Phat et al. 2022). A total of 25 components were identified in the MAHD process on *Citrus hystrix* leaves, which are presented in Table 15. The five most frequently detected compounds were citronellal (70.39%), citronellol (14.33%), linalool (2.75%), citronellyl isobutyrate (2.02%), and caryophyllene (1.84%). The high level of oxygenated compounds is responsible for the odorous properties of essential oils. Besides, monoterpenes such as citronella have biological properties and effects: antinociceptive and anti-inflammatory (Astuti et al. 2022). Citronella oil was also identified in *Cymbopogon nardus* leaves (9.67%); it was one of the highest amounts of volatile compounds (Haqqyana et al. 2022). In another study, *Citrus hystrix* leaves from East Borneo had 77.29% of the main compound citronella in fresh leaves, which was similar to this study. The decrease in citronella compounds also occurred in dry leaves (Naibaho et al. 2024). The amounts of citronella and other compounds in *Citrus hystrix* vary based on geographical conditions. In previous studies, it was reported that the amount of citronella was higher compared to Malaysia and Thailand (Hien et al. 2020a). The different extraction methods for essential oils vary in the type and amount of compounds. There were 15 and 13 volatile compounds detected in hydrodistillation and steam-distillation. A high amount of citronella was detected by hydro-distillation and steam-distillation methods. In contrast, the citronellol amount in this study was higher than the conventional method, which is shown in Table 13. Other chemical contents were detected in the MAHD process, such as 2-hexenal, ß-phellandrene, ß-ocimene, and humulene. Limonene compounds had an effect on increasing spiciness, taste, and aroma (Ngan et al. 2019; Quyen et al. 2020; Hien et al. 2020b). So, essential oil compounds that are extracted by the MAHD process are more complex compared to hydro-distillation and steam-distillation. The integrity of the essential oil compounds during the MAHD process was verified to ensure that no significant degradation occurred. GC–MS analysis consistently identified citronellal and citronellol as the dominant constituents, which is in agreement with the typical composition of *Citrus hystrix* essential oil (Fig. 11). Furthermore, the FTIR spectra did not show additional unexpected peaks that could indicate thermal degradation products. These findings confirm that the MAHD process was able to extract essential oils effectively while maintaining the stability of the major volatile compounds.

Figures 12 and 13 show SEM analysis, which identified the morphology structure of the leaves with 1000–8000 × magnification. Before the MAHD process was carried out, the cell walls of *Citrus hystrix* leaves were tightly and neatly packed, which can be seen in Fig. 12. In contrast, changes in the physical structure of the *Citrus hystrix* leaf samples were clearly damaged after extraction. The movement of molecules around the leaves and the solvent caused the microwave to harm the *Citrus hystrix* leaf samples. The microwave heating intensity damages cell walls and reduces surface tension. The existence of cavities in the *Citrus hystrix* leaves at 4000 × and 8000 × magnification indicates morphological deterioration. The diffusion of the material's essential oils into the solvent is demonstrated by the damage and voids in Fig. 13 (Nurhadi et al. 2022; Alara et al. 2019; Singh et al. 2022).

4 Conclusion

This research explores the optimization and kinetics of *Citrus hystrix* leaf extraction using microwave hydrodistillation. Optimization was determined by RSM using BBD and FCCCD design with variable parameters: the power of microwave (W), the F/S ratio (g/ml), and the extraction time (minutes). The predicted yields were 1.367% for the BBD design and 1.426% for the FCCCD design, with residuals of 0.01151% and − 0.03619%, respectively. Further, the kinetics study uses an empirical model to estimate the extraction mechanism. The suitable models of the MAHD process on *Citrus hystrix* leaves were the first-order model and the Peleg model because the coefficient of determination (R^2) was close to 1, and the RSME value was close to 0. The value of k and the extraction rate were extrapolated

Table 15 Comparison of GC–MS results analysis for each extraction method

No	Compounds	Content (%)		
		This study	Hydro-distillation (Hien et al. 2020b)	Steam-distillation (Quyen et al. 2020)
1	2-Hexenal	0.20	-	-
2	ß-Phellandrene	1.25	-	-
3	ß-Pinene	0.50	0.311	-
4	D-Limonene	0.16	0.34	0.401
5	ß-Ocimene	0.31	-	-
6	Sabinene	-	0.744	1.004
7	Linalool	2.75	1.891	1.622
8	Citronellal	70.39	85.436	86.89
9	1-Dodecyn-4-ol	0.40	-	-
10	Citronellol	14.33	6.808	4.899
11	Geraniol	0.89	-	-
12	Cyclohexanol	-	0.657	
13	Citronellic acid	0.27	-	-
14	p-Menthane-3,8-diol, cis-1,3,trans-1,4-	0.79	-	-
15	Citronellyl isobutyrate	2.02	-	-
16	Copaene	0.78	0.211	0.263
17	cis-Muurola-4(15),5-diene	0.30	-	-
18	Caryophyllene	1.84	1.012	0.956
19	Humulene	0.23	-	-
20	Germacrene D	0.15	-	-
21	elemene	0.20	0.092	-
22	Citronellyl acetate	-	1.705	2.919
23	Isoledene	0.68	-	-
24	Geranyl acetate	-	-	0.036
25	cubebene	-	0.133	0.23
26	Nerolidol	0.84	-	-
27	Caryophyllene oxide	0.23	-	0.36
28	Globulol	0.17	-	-
29	Isospathulenol	0.17	-	-
30	Cyclohexane	-	0.191	0.09
31	Naphthalene	-	0.283	-
32	Cadinene	-	-	0.331
33	Elemol	-	0.185	-
34	Thunbergol	0.15	-	-

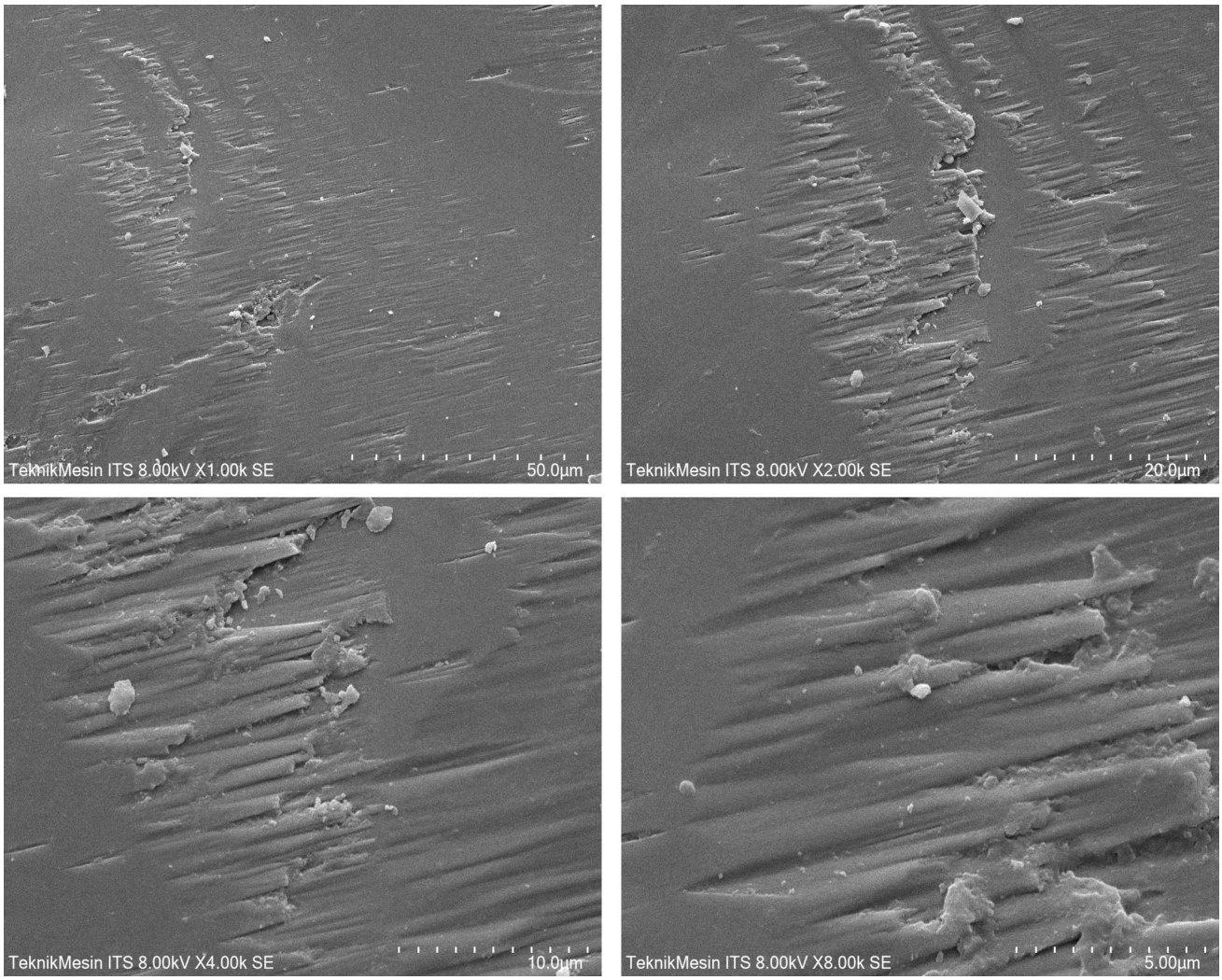


Fig. 12 SEM analysis of *Citrus hystrix* leaves before the MAHD process

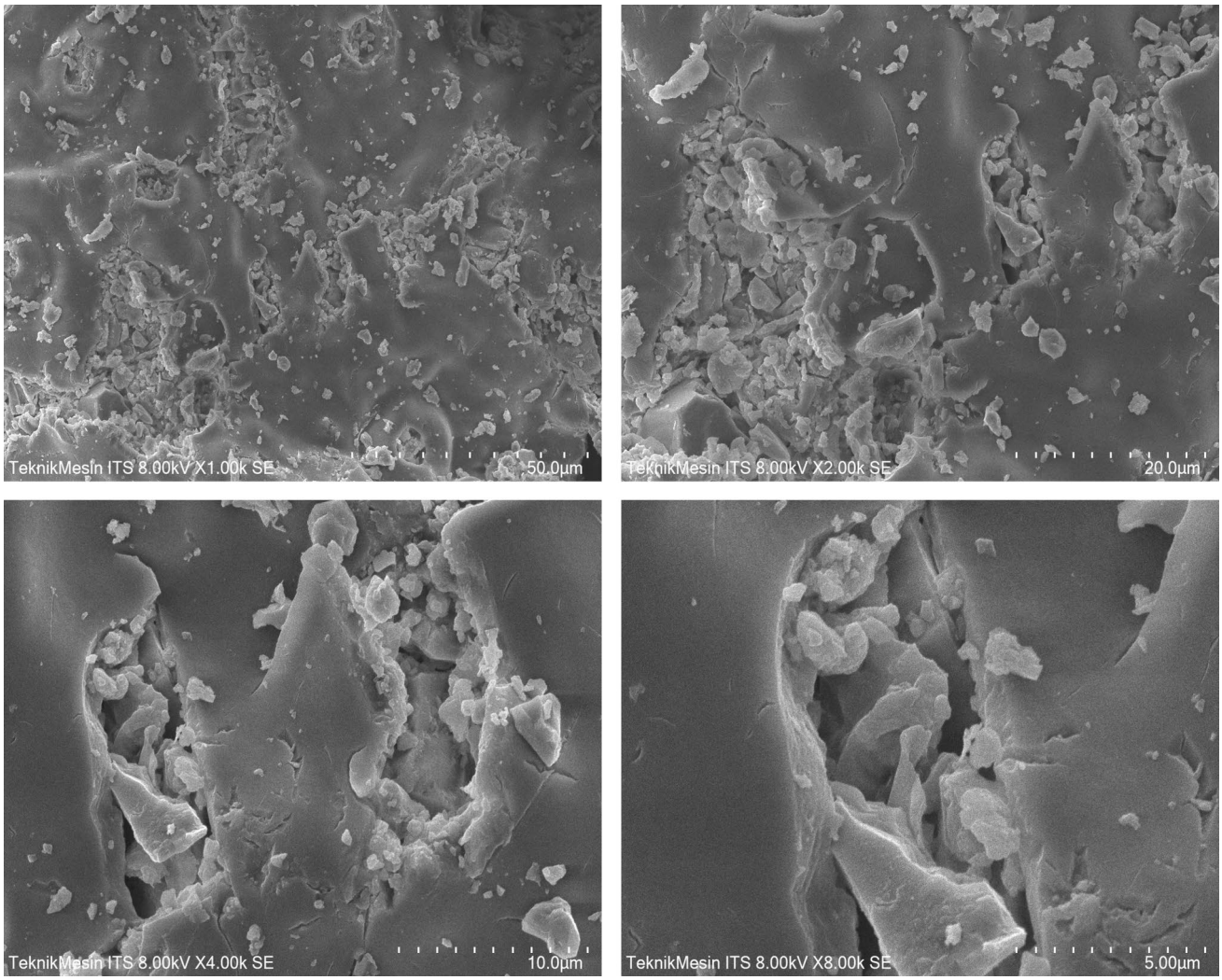


Fig. 13 SEM analysis of *Citrus hystrix* leaves after the MAHD process

by mathematical equations. The mathematical equation of the first-order kinetics model was more suitable to predict the value of each F/S ratio than the Peleg kinetics model ($R^2 = 0.97–0.99$ and RSME = 0.0013–0.0021). The results of FTIR analysis showed that the essential oil extract was similar to the citronellal compound (93.69%). GC–MS analysis also showed that the most common essential oil extract components were citronellal (70.39%) and citronellol (14.33%).

Acknowledgements We gratefully acknowledge the support of Politeknik ATI Makassar for providing access to laboratory facilities and necessary materials.

Author contribution Dwi Setyorini and Achmad Qodim Syafaatullah investigated, analyzed data, wrote and revised the manuscript. Novita Ramadhani, Silvana Zaimul, and Sitti Khusnul Khotimah did experiment and reviewed. Anggi Yuktii Kulla, Frabowo Prasetya, and Sabdha Purna Yudha analyzed data, edited, and reviewed.

Funding This research funding was provided by the Educational Unit of the Ministry of Industry via the program "Sarana Penelitian Industri Terapan."

Data availability All datasets generated and/or analyzed during the present study are included in this published article. Additional supporting data are available from the corresponding author on reasonable request.

Declarations

Conflict of interest The authors declare no competing interests.

Open Access This article is licensed under a Creative Commons Attribution 4.0 International License, which permits use, sharing, adaptation, distribution and reproduction in any medium or format, as long as you give appropriate credit to the original author(s) and the source, provide a link to the Creative Commons licence, and indicate if changes were made. The images or other third party material in this article are included in the article's Creative Commons licence, unless indicated otherwise in a credit line to the material. If material is not included in the article's Creative Commons licence and your intended use is not

permitted by statutory regulation or exceeds the permitted use, you will need to obtain permission directly from the copyright holder. To view a copy of this licence, visit http://creativecommons.org/licenses/by/4.0/.

References

Alara OR, Abdurahman NH, Ukaegbu CI, Kabbashi NA (2019) Extraction and characterization of bioactive compounds in *Vernonia amygdalina* leaf ethanolic extract comparing Soxhlet and microwave-assisted extraction techniques. J Taibah Univ Sci 13(1):414–422. https://doi.org/10.1080/16583655.2019.1582460

Astuti IP, Palupi KD, Damayanti F (2022) Essential oils composition of kaffir lime (Citrus hystrix DC.) collection of Bogor Botanic Gardens from Central Java and East Sumba. J Trop Biodivers Biotechnol 7(1). https://doi.org/10.22146/JTBB.66061

Athanasiadis V, Chatzimitakos T, Bozinou E, Kotsou K, Palaiogiannis D, Lalas SI (2023) Optimization of extraction parameters for enhanced recovery of bioactive compounds from quince peels using response surface methodology. Foods 12(11). https://doi.org/10.3390/foods12112099

Chen F, Guo Y, Kang J, Yang X, Zhao Z, Liu S, Ma Y, Gao W, Luo D (2020) Insight into the essential oil isolation from *Foeniculum vulgare* Mill. fruits using double-condensed microwave-assisted hydrodistillation and evaluation of its antioxidant, antifungal and cytotoxic activity. Ind Crops Prod 144:112052. https://doi.org/10.1016/j.indcrop.2019.112052

Das I, Arora A (2021) Kinetics and mechanistic models of solid-liquid extraction of pectin using advance green techniques- a review. Food Hydrocoll 120:01. https://doi.org/10.1016/j.foodhyd.2021.106931

Didar Z, Hesarinejad MA (2022) Preparation of vitamin D3-loaded oil-in-water-in-oil double emulsions using psyllium gum: optimization using response surface methodology. Chem Biol Technol Agric. https://doi.org/10.1186/s40538-022-00348-6

Drinić Z, Pljevljakušić D, Živković J, Bigović D, Šavikin K (2020) Microwave-assisted extraction of *O. vulgare* L. spp. hirtum essential oil: comparison with conventional hydro-distillation. Food Bioprod Process 120:158–165. https://doi.org/10.1016/j.fbp.2020.01.011

Dulo B, De Somer T, Moyo M, Nakyese E, Githaiga J, Raes K, De Meester S (2023) Kinetic modeling of phenolic compounds extraction from nutshells: influence of particle size, temperature and solvent ratio. Biomass Convers Biorefin. https://doi.org/10.1007/s13399-023-04993-1

Golmohammadi M, Borghei A, Zenouzi A, Ashrafi N, Taherzadeh MJ (2018) Optimization of essential oil extraction from orange peels using steam explosion. Heliyon 4(11):e00893. https://doi.org/10.1016/j.heliyon.2018.e00893

Haqqyana H, Altway A, Mahfud M (2022) Kinetic modeling for microwave-assisted green extraction: effects of power on citronella oil from *Cymbopogon nardus* leaf. Int J Appl Sci Eng. https://doi.org/10.6703/IJASE.202212_19(4).007

Hien TT, Quyen NTC, Minh PTH, Le XT (2020) Determine the components of kaffir lime oil (Citrus Hystrix DC.) in the microwave-assisted extraction process. In IOP Conference Series: Materials Science and Engineering 991(1). https://doi.org/10.1088/1757-899X/991/1/012018

Hien TT, Quyen NTC, Truc TT, Quan PM (2020) Evaluate the chemical composition of Kaffir lime (Citrus hystrix) essential oil using the classical method. In IOP Conference Series: Materials Science and Engineering 991(1). https://doi.org/10.1088/1757-899X/991/1/012014

Karabegoić I, Stojanović SS, Mančić S, Đorđević N, Malićanin M, Danilović B (2023) Optimization of food-grade bioactive compound extraction from plant sources by response surface methodology approach: a comprehensive review. MASO INTERNATIONAL – JOURNAL OF FOOD SCIENCE AND TECHNOLOGY 13(1):31–47. https://doi.org/10.2478/mjfst-2023-0004

Kusuma HS, Mahfud M (2017) The extraction of essential oils from patchouli leaves (*Pogostemon cablin* Benth) using a microwave air-hydrodistillation method as a new green technique. RSC Adv 7(3):1336–1347. https://doi.org/10.1039/C6RA25894H

Letchumanan K, Abdullah NH, Pisar MM, Ismail HM, Kadir R, Abdul-Aziz A (2023) Application of response surface methodology for the optimization of the extraction of triterpenoid saponins from Azadirachta excelsa leaves. Chem Eng Trans 106:1159–1164. https://doi.org/10.3303/CET23106194

Lis MJ, García Carmona Ó, Carmona CG, Bezerra FM (2018) Inclusion complexes of citronella oil with β-cyclodextrin for controlled release in biofunctional textiles. Polymers (Basel) 10 Nov. 2018, [Online]. Available: www.mdpi.com/journal/polymersrticle

Maharaj S, McGaw D (2020) Mathematical model for the removal of essential oil constituents during steam distillation extraction. Processes 8(4). https://doi.org/10.3390/PR8040400

Mahfud M, Haqqyana H, Finish V, Tania W, Suyadi AM, Septya Kusuma H, Altway A (2020) Moroccan Journal of Chemistry Kinetic study in the extraction of essential oil from clove (Syzgium aromaticum) stem using microwave hydrodistillation. Moroccan J Chem, Jan. 2020, [Online]. Available: http://revues.imist.ma/?journal=morjchem&page=login

Mas'Ud F, Mahendradatta M, Laga A, Zainal Z (2017) Optimization of mango seed kernel oil extraction using response surface methodology. OCL - Oilseeds fats, Crops Lipids 24(5). https://doi.org/10.1051/ocl/2017041

Megawati DS, Fardhyanti WB, Sediawan A, Hisyam A (2019) Kinetics of mace (*Myristicae arillus*) essential oil extraction using microwave assisted hydrodistillation: effect of microwave power. Ind Crops Prod 131:315–322. https://doi.org/10.1016/j.indcrop.2019.01.067

Menkiti M, Agu CM (2019) Extraction kinetics and physicochemical studies of Terminalia catappa L kernel oil utilization potential. J Chem Chem Eng Res Artic 38(3)

Messadi N, Mechmeche M, Setti K, Tizemmour Z, Hamdi M, Kachouri F (2023) Optimization of extraction parameters and characterization of Tunisian date extract: a scientific approach toward their utilization. Sugar Tech 25(2):460–472. https://doi.org/10.1007/s12355-022-01223-2

Mohammadhosseini M, Sarker SD, Akbarzadeh A (2017) Chemical composition of the essential oils and extracts of *Achillea* species and their biological activities: a review. J Ethnopharmacol 199:257–315. https://doi.org/10.1016/j.jep.2017.02.010

Murni SW, Setyoningrum TM, Cahyaningrum FXDD, Alodia S, Kusuma HS (Dec.2021) Extraction of citronella oil (Cymbopogon winterianus Jowitt) using hydrodistillation method: the effect of F/S ratio and extraction time. RSF Conference Series: Engineering and Technology 1(1):319–323. https://doi.org/10.31098/cset.v1i1.389

Naibaho NM, Safitri ASM, Rudito, Popang EP, Syauqi A, Saragih B, Amirta R, Arung ET (2024) Chemical composition and antibacterial activity of essential oil kaffir lime (Citrus hystrix DC) leaves from East Borneo. Food Res 8(1):250–256. https://doi.org/10.26656/fr.2017.8(1).100

Natolino A, Da Porto C (2020) Kinetic models for conventional and ultrasound assistant extraction of polyphenols from defatted fresh and distilled grape marc and its main components skins and seeds. Chem Eng Res Des 156:1–12. https://doi.org/10.1016/j.cherd.2020.01.009

Ngan TTK, Hien TT, Le XT, Anh TT, Quan PM, Cang MH, Le Ngoc TT, Danh VT, Yen Trung LN, Toan TQ (2019) Physico-chemical profile of essential oil of Kaffir lime (*citrus hystrix* DC) grown in An Giang Province, Vietnam. Asian J Chem 31(12):2855–2858. https://doi.org/10.14233/ajchem.2019.22167

Nurhadi B, Angiputri FC, Andoyo R, Ermawar RA, Saputra RA (2022) Antioxidant stability of moringa leaves extract powders obtained

by cocrystallization, vacuum drying, and plating. J Food Qual. https://doi.org/10.1155/2022/3038403

Phat T, Van M, Ngoc Q, Le T, Tran N, Yen T, Van T (2022) Experimental and kinetic modeling studies on extraction. Chem. Eng. Research Article 41(11):2022

Prasetyaningrum A, Ratnawati R, Hargono H, Haryani K, Wicaksono BS, Hakiim A, Annafi RD, Ashianti AD (2024) Ultrasound-assisted encapsulation of citronella oil (*Cymbopogon nardus*) in alginate/carrageenan beads using ionic gelation method. Food Res 8:60–66. https://doi.org/10.26656/fr.2017.8(S1).9

Quyen NTC, Ngan TTK, Phong HX, Hien TT, Dung LT (2020) Extraction of Kaffir Lime (Citrus hystrix DC.) essential oil by steam distillation and evaluation of chemical constituents. In IOP Conference Series: Materials Science and Engineering 991(1). https://doi.org/10.1088/1757-899X/991/1/012015

Ragab TIM, El Gendy ANG, Saleh IA, Esawy MA (2019) Chemical composition and evaluation of antimicrobial activity of the Origanum majorana essential oil extracted by microwave-assisted extraction, conventional hydro-distillation and steam distillation. J Essent Oil-Bear Plants 22(2):563–573. https://doi.org/10.1080/0972060X.2019.1611486

Raji Z, Kiani H (2020) Kinetic modeling of pectin extraction by ultrasound assisted and conventional methods. J Food Bioprocess Eng 3:121–127. https://doi.org/10.22059/jfabe.2020.308224.1061

Rusydan AM, Lukitaningsih E, Fakhrudin N (2021) Modeling and optimization of *Mitragyna speciosa* extraction using Box Behnken design. Maj Obat Tradis 26(3):204–210. https://doi.org/10.22146/mot.68610

Singh P, Mishra S, Bhimrao Ambedkar B (2022) Qualitative phytochemical screening and elemental analysis of Thai basil leaves using SEM-EDS, XRD. YMER 21(6):1055–1065, Jun. 2022, [Online]. Available: http://ymerdigital.com

Songkro S, Hayook N, Jaisawang J, Maneenuan D, Chuchome T, Kaewnopparat N (2012) Investigation of inclusion complexes of citronella oil, citronellal and citronellol with b-cyclodextrin for mosquito repellent. J Incl Phenom Macrocycl Chem 72(3–4):339–355. https://doi.org/10.1007/s10847-011-9985-7

Syafaatullah AQ, Setyorini D, Ganing M, Panjaitan R, Azizah N (2023) Optimization and kinetics extraction of natural dyes from henna leaves (*Lawsonia inermis* L.) with ultrasonic assistance. J Kim Sains Dan Apl 26(9):324–331. https://doi.org/10.14710/jksa.26.9.324-331

Wang Y, Wang C, Xue H, Jin Y, Yang M, Leng F (2023) Comparative analysis of three kinds of extraction kinetic models of crude polysaccharides from Codonopsis pilosula and evaluate the characteristics of crude polysaccharides. Biomass Convers Biorefin 13(14):12917–12933. https://doi.org/10.1007/s13399-022-02518-w

Zafirah Mohd Sopi N, Hazwan bin Hamzah M, Che Man H, Nor Z, Sopi NZM, Hamzah MH, Man HC, Nor MZM, Radzuan MN, Author C (2021) Process optimization of ultrasonic-assisted-soxhlet-extraction of essential oil from Citrus hystrix using response surface methodology. AMA Agric Mech Asia Africa Lat Am 52(3):4043–4061

Publisher's Note Springer Nature remains neutral with regard to jurisdictional claims in published maps and institutional affiliations.